AIP Journal of Applied Physics

Room-temperature tunable microwave properties of strained Sr Ti O 3 films

Wontae Chang, Steven W. Kirchoefer, Jeffrey M. Pond, Jeffrey A. Bellotti, Syed B. Qadri, Jeffrey H. Haeni, and Darrell G. Schlom

Citation: Journal of Applied Physics **96**, 6629 (2004); doi: 10.1063/1.1813641
View online: http://dx.doi.org/10.1063/1.1813641
View Table of Contents: http://scitation.aip.org/content/aip/journal/jap/96/11?ver=pdfcov
Published by the AIP Publishing

Articles you may be interested in
An electrode-free method of characterizing the microwave dielectric properties of high-permittivity thin films
J. Appl. Phys. **109**, 024106 (2011); 10.1063/1.3537835

Influence of applied electric field annealing on the microwave properties of (Ba 0.5 Sr 0.5) Ti O 3 thin films
Appl. Phys. Lett. **90**, 162905 (2007); 10.1063/1.2727560

MgO-mixed Ba 0.6 Sr 0.4 TiO 3 bulk ceramics and thin films for tunable microwave applications
J. Appl. Phys. **92**, 3941 (2002); 10.1063/1.1505669

Strain-relieved Ba 0.6 Sr 0.4 TiO 3 thin films for tunable microwave applications
J. Appl. Phys. **92**, 1528 (2002); 10.1063/1.1491996

The effect of annealing on the microwave properties of Ba 0.5 Sr 0.5 TiO 3 thin films
Appl. Phys. Lett. **74**, 1033 (1999); 10.1063/1.123446

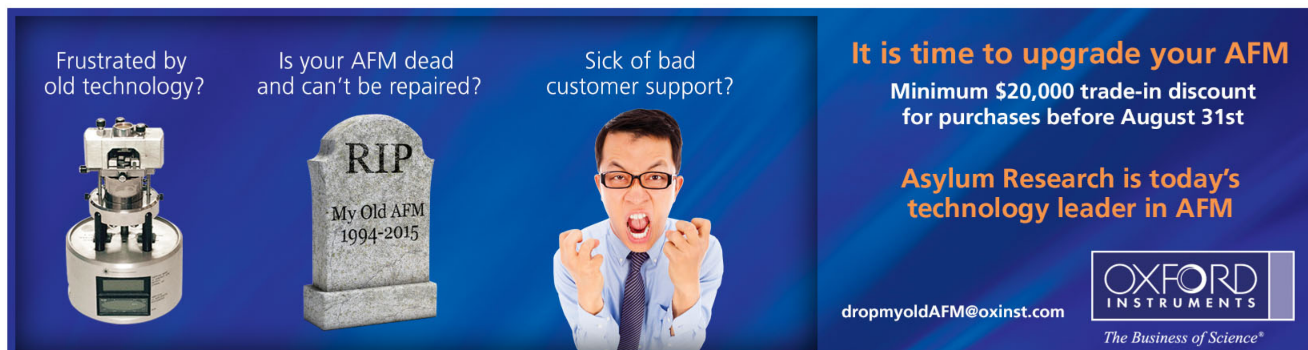

[This article is copyrighted as indicated in the article. Reuse of AIP content is subject to the terms at: http://scitation.aip.org/termsconditions. Downloaded to] IP: 128.84.143.26 On: Tue, 16 Jun 2015 17:09:37

HTML ABSTRACT + LINKS

JOURNAL OF APPLIED PHYSICS VOLUME 96, NUMBER 11 1 DECEMBER 2004

Room-temperature tunable microwave properties of strained $SrTiO_3$ films

Wontae Chang,[a)] Steven W. Kirchoefer, Jeffrey M. Pond, Jeffrey A. Bellotti, and Syed B. Qadri
Naval Research Laboratory, Washington, DC 20375

Jeffrey H. Haeni and Darrell G. Schlom
Pennsylvania State University, University Park, Pennsylvania 16802

(Received 6 July 2004; accepted 14 September 2004)

Structural distortion of ferroelectric thin films caused by film strain has a strong impact on the microwave dielectric properties. $SrTiO_3$ thin films epitaxially grown on (110) $DyScO_3$ substrates using molecular beam epitaxy are extremely strained (i.e., ~1% in-plane tensional strain) from 3.905 Å of bulk $SrTiO_3$. The room-temperature in-plane dielectric constant and its tuning of the films at 10 GHz are observed to be 6000 and 75% with an electric field of 1 V/μm, respectively. The control of strain in $SrTiO_3$ provides a basis for room-temperature tunable microwave applications by elevating its phase-transition peak to room temperature. © *2004 American Institute of Physics*. [DOI: 10.1063/1.1813641]

I. INTRODUCTION

The dc electric-field-dependent dielectric constant of ferroelectric thin films, such as $Ba_{1-X}Sr_XTiO_3$ (BST, $0 \leqslant X \leqslant 1$), is currently being used to develop high dielectric Q ($=1/\tan\delta$) tunable microwave devices, such as voltage-controlled oscillators, tunable filters, and phase shifters.[1–3] The Curie temperature (T_C) of the bulk BST varies almost linearly with the composition, X, in the solid solution $Ba_{1-X}Sr_XTiO_3$. For a particular application temperature, the composition is adjusted to move the ferroelectric phase transitions to the range of the device application temperature. Normally, $Ba_{0.5}Sr_{0.5}TiO_3$ and $Ba_{0.6}Sr_{0.4}TiO_3$, whose phase transitions are 250 and 280 K, respectively, are used for a room-temperature application because they are paraelectric phases (i.e., low dielectric loss), but still show nonlinear dielectric properties (i.e., high dielectric tuning) at room temperature. $SrTiO_3$ (i.e., $Ba_{1-X}Sr_XTiO_3$, $X=1$) is known as an incipient ferroelectric material, whose ferroelectric phase transition is suppressed by quantum fluctuations and whose nonlinear dielectric properties are exhibited only at very low temperatures (i.e., below 65 K).[4–6] Therefore, it has been considered only for low-temperature applications.[7]

Strain is one of the important factors affecting the ferroelectric properties because the strain is directly coupled with the ionic polarization in a ferroelectric.[8–11] It has been demonstrated that strain affects the ferroelectric phase transition, the dielectric constant, and the dielectric tuning.[12–17] For compressive strain, the ferroelectric phase-transition peak shifts to a lower temperature, resulting in a decreased dielectric constant and tuning, whereas for tensional strain, the opposite effect is observed. Recently, extremely strained (~1% tensional strain) but unit-cell level smooth epitaxial $SrTiO_3$ films have been successfully deposited on (110) $DyScO_3$ substrates using a molecular beam epitaxy (MBE) at Pennsylvania State University[18,19] (i.e., normally, ~1% strain is known as a fracture strain for oxide materials). In this article, the film structure and microwave dielectric properties for highly strained $SrTiO_3$ films are analyzed and characterized for room-temperature tunable microwave applications.

II. EXPERIMENT

$SrTiO_3$ thin films of various thicknesses (100-, 200-, 300-, 500-, and 1000-Å thick) have been deposited onto (110) $DyScO_3$ single-crystal substrates at 650 °C by molecular beam epitaxy.[18,19] $DyScO_3$ crystal substrate is a $LnMO_3$ orthorhombic structure (Pbnm) (Refs. 20 and 21) with anisotropic dielectric properties (Table I). A continuous flux of molecular oxygen mixed with 10% ozone was controlled to yield a background pressure of 5.0×10^{-7} Torr. The average incident flux of both the Sr and Ti sources was maintained constant at 1.0×10^{14} $cm^{-2}\,s^{-1}$ to achieve a layer-by-layer growth of Sr and Ti in a sequential manner. Reflection high-energy electron diffraction (RHEED) intensity oscillations were used to adjust the stoichiometry of the Sr and Ti molecular beams and ensure that a complete monolayer of each cation was deposited in each shuttered cycle (i.e., 6.6×10^{14} atoms/cm^{-2} of the monolayer doses).[18] X-ray diffraction (XRD) and atomic force microscopy (AFM) were used for film structure and surface morphology characterization.

Interdigitated capacitors (IDC) were deposited on top of the $SrTiO_3$ films (100-, 200-, 500-, and 1000-Å thick) through a polymethylmethacrylate lift-off mask by e-beam evaporation of 1.5-μm-thick Ag with an adhesive thin layer

TABLE I. The lattice parameter and dielectric constant of the $DyScO_3$ single-crystal substrate.

Lattice parameter[a]		Dielectric constant[b]	
a	5.440 Å	ε_{11}	22.0
b	5.713 Å	ε_{22}	18.8
c	7.887 Å	ε_{33}	35.5

[a]Reference 21.
[b]Reference 19.

[a)]Electronic mail: chang@estd.nrl.navy.mil

 © 2004 American Institute of Physics

[This article is copyrighted as indicated in the article. Reuse of AIP content is subject to the terms at: http://scitation.aip.org/termsconditions. Downloaded to] IP: 128.84.143.26 On: Tue, 16 Jun 2015 17:09:37

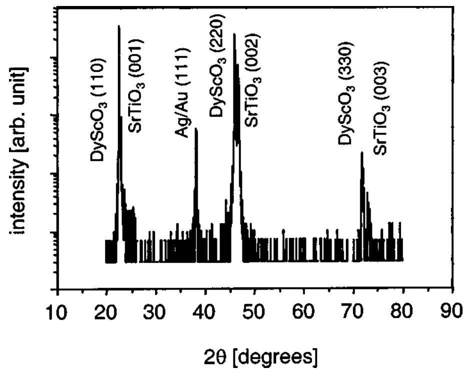

FIG. 1. A typical XRD pattern of $SrTiO_3$ thin films deposited on (110) $DyScO_3$ substrates.

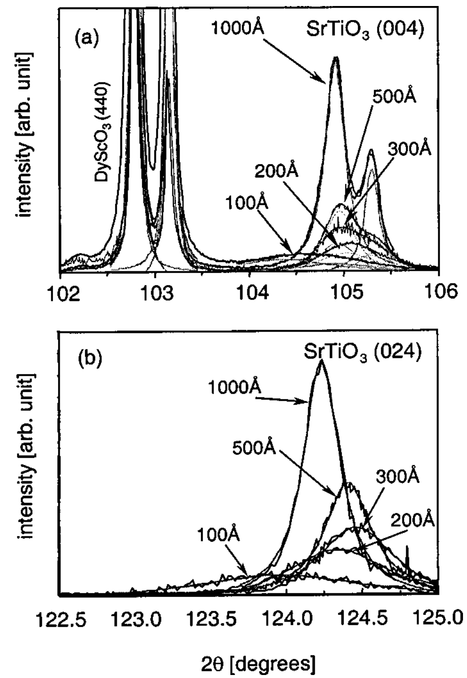

FIG. 2. XRD patterns of (a) symmetric (004) peaks and (b) asymmetric (024) peaks of $SrTiO_3$ thin films deposited on (110) $DyScO_3$ with different film thickness.

of Cr and a protective thin layer of Au. The microwave dielectric properties, capacitance, and device Q of the $SrTiO_3$ thin films, were measured as a function of frequency (45 MHz–20 GHz), dc bias voltage (–40 to 40 V), and temperature (10 to 330 K). S_{11} measurements were made using interdigitated capacitors probed by a 200-μm pitch Picoprobe microwave probe, which was connected to an HP 8510C network analyzer. The measured S_{11} data were fitted to a parallel resistor-capacitor model to determine the capacitance and device Q of the films. The dielectric constant and dielectric loss (tan δ) of the films was extracted from the device capacitance, the device Q, and the IDC capacitor dimensions through a conformal mapping technique.[22]

III. RESULTS AND DISCUSSION

A. Film structure and surface morphology

Figure 1 shows a θ-2θ XRD scan for $SrTiO_3$ thin film (1000-Å thick) deposited onto (110) $DyScO_3$ single-crystal substrates at 650 °C by MBE. As shown in the figure, the normal direction to the surface of the $SrTiO_3$ films is only [001] $SrTiO_3$. Also, a Ag/Au peak from the electrodes deposited onto the film appears in the XRD pattern. For these [001]-oriented $SrTiO_3$ films (100-, 200-, 300-, 500-, and 1000-Å thick), the lattice parameters along the surface normal ($a_\perp$) and in the plane of the films ($a_\parallel$) were determined from the XRD patterns of symmetric (004) and asymmetric (024) reflections (Fig. 2). In cases where the XRD peak intensity from the films was not clear enough to determine the peak position, the XRD summation mode was used. Also, the diffraction pattern for asymmetric (024) reflections was obtained from a monochromatic x-ray source ($K\alpha_1$ only) generated using a Ge(111) crystal. Diffraction peaks from the $DyScO_3$ substrate with the $SrTiO_3$ (004) reflections were used as an internal standard to reduce errors associated with measurement. Each $SrTiO_3$ (004) diffraction peak was fitted with two Gaussian functions by considering four factors of peak shape (the ratios of height, width, area of $K\alpha_1$ and $K\alpha_2$ peaks, and the distance between $K\alpha_1$ and $K\alpha_2$ peaks) after removing the background, while the $SrTiO_3$ (024) diffraction peak was fitted with one Gaussian function. It is worth noting that the asymmetric $SrTiO_3$ (024) reflections were obtained only after the substrate was rotated by 45° and 135° in the substrate plane with respect to the substrate edge, indicating that the edge of $SrTiO_3$ unit cell is rotated 45° and 135° from the substrate edge in these particular substrates.

The lattice parameters of the $SrTiO_3$ thin films calculated from an analysis of the XRD data (with the exception of the 100-Å-thick $SrTiO_3$ film) are presented in Table II. The XRD peak for the 100-Å-thick $SrTiO_3$ film is too weak and broad to determine the peak position because the film thickness is too thin (Fig. 2). As shown in Table II, the normal lattice parameter is compressed and the in-plane lattice parameter of $SrTiO_3$ films is extended from the 3.905 Å value of bulk $SrTiO_3$. A measurement error greater than ±0.001 Å in the lattice parameter in Table II arises from an uncertainty in the fitting procedure to determine the peak position, which is mainly due to insufficient XRD peak intensities for very thin films (i.e., ⩽500-Å thick), even though a sufficient number of scans (i.e., 10~20 scans) is used in the XRD summation mode; and possibly due to a broader distribution in the lattice parameter as the film thickness is reduced. Table II shows a higher uncertainty in the in-plane lattice parameter than the normal lattice parameter because of the weaker and broader XRD peaks for the in-plane lattice parameter (Fig. 2). Table III shows the film strains from the measured lattice parameters, and also includes the in-plane

TABLE II. The lattice parameter of $SrTiO_3$ films with different film thicknesses and the corresponding XRD peak widths in 2theta.

Thickness [Å]	a_{normal} [Å]	FWHM($k\alpha_1$) [degrees]	$a_{\text{in-plane}}$ [Å]	FWHM($k\alpha_1$) [degrees]
1000	3.883±0.001	0.2	3.941±0.001	0.3
500	3.882±0.001	0.3	3.932±0.002	0.4
300	3.882±0.002	0.4	3.931±0.003	0.7
200	3.881±0.002	0.5	3.937±0.004	0.9

[This article is copyrighted as indicated in the article. Reuse of AIP content is subject to the terms at: http://scitation.aip.org/termsconditions. Downloaded to] IP: 128.84.143.26 On: Tue, 16 Jun 2015 17:09:37

TABLE III. $SrTiO_3$ film strains with different film thicknesses.

Thickness [Å]	Normal strain (XRD)	In-plane strain (Estimation[a])	In-plane strain (XRD)
1000	−0.0056	0.0098	0.0092
500	−0.0059	0.0102	0.0069
300	−0.0059	0.0102	0.0067
200	−0.0062	0.0106	0.0082

[a]Estimated in-plane strain from measured normal strain with $x_{1,2}=-x_3(C_{11}/2C_{12})$, where $x_{1,2}$, x_3, and C are in-plane, normal film strain, and elastic constants for $SrTiO_3$.

strain estimated from the normal strain based on XRD data, which shows higher accuracy (Tables II and III). The in-plane lattice parameter of the films is extremely extended from the 3.905 Å value of bulk $SrTiO_3$ (i.e., ~1%).

Figure 3 shows an AFM image of a $SrTiO_3$ film (200-Å thick). The film surface is extremely smooth with a surface rms roughness of 3.880 Å, which is approximately the same as one unit cell of the $SrTiO_3$ film (Table I). The grain size is about 400~500 Å. Figure 3 shows typical AFM images for the other $SrTiO_3$ films (i.e., 300-, 500-, and 1000-Å thick). It is worth noting that the severely strained (i.e., ~1%) $SrTiO_3$ films are still in an elastic region without any fracture even though ~1% strain is a typical fracture strain for oxide materials, presumably due to the fact that the films have a high degree of uniformity and structural perfection resulted from an extremely small lattice mismatch (i.e., ~1%) with $DyScO_3$ single-crystal substrates and a well-controlled layer-by-layer film growth using a reactive MBE equipped with RHEED.[18,19]

B. Microwave dielectric properties

Figure 4(a) shows the dielectric constant of $SrTiO_3$ thin films (500-Å thick) as a function of applied dc bias measured at 10 GHz and room temperature. The as-deposited $SrTiO_3$ film exhibits a huge dielectric constant (i.e., ~6000) and a large dielectric tuning (i.e., ~85% at 4 V/μm) at room temperature. It is also interesting to note that most of the dielectric tuning of as-deposited $SrTiO_3$ film occurs at a low dc bias field (i.e., ~75% at 1 V/μm). Such a high dielectric tuning with a large dielectric constant of $SrTiO_3$ films at 300 K in Fig. 4(a) is comparable to the previously reported

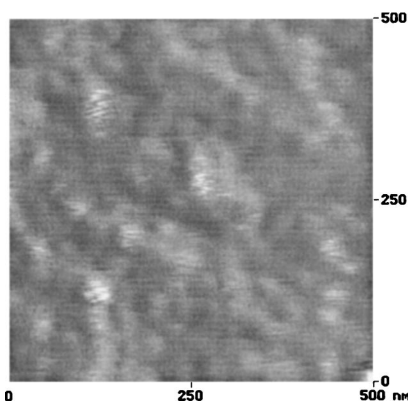

FIG. 3. An AFM image of $SrTiO_3$ film (200-Å thick).

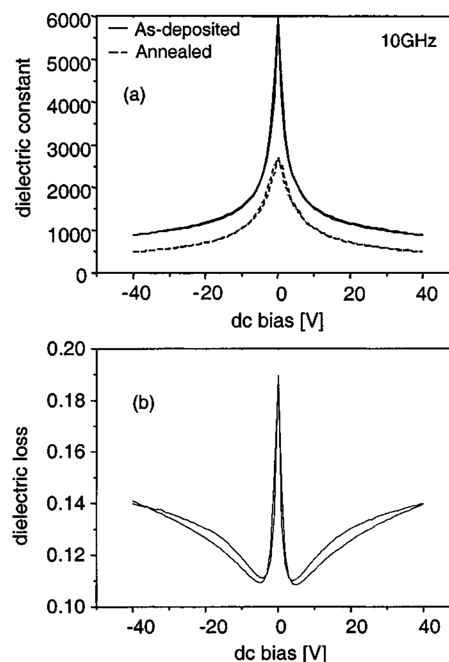

FIG. 4. Room-temperature (a) dielectric constant of $SrTiO_3$ thin films (500-Å-thick as-deposited and annealed) and (b) dielectric loss (tan δ) of the as-deposited film at 10 GHz (gap=6 μm).

low-temperature dielectric properties of $SrTiO_3$ single crystals, showing an 88% dielectric tuning at 2 V/μm and a dielectric constant of 15 000 at 30 K.[5] However, at 300 K, the dielectric properties of $SrTiO_3$ crystals reported 0% dielectric tuning with a dielectric constant of 400.[5] As shown in Fig. 4(a), the annealing effect is critical on the dielectric properties as the annealed film (i.e., for 30 min at 700 °C in atmosphere) shows a significantly reduced dielectric constant (i.e., ~2500) and dielectric tuning (i.e., ~60% at 1 V/μm).

Figure 5(a) shows the capacitance and device Q of annealed $SrTiO_3$ films (500-Å thick) as a function of temperature and dc bias (i.e., 0 V for solid lines and 40 V for dotted lines) measured at 10 GHz. Figure 5(a) also includes the capacitance of as-deposited $SrTiO_3$ films (500-Å thick) plotted with thicker lines. Figure 5(b) shows the capacitance of annealed $SrTiO_3$ films (100-Å and 200-Å thick) as a function of temperature and dc bias measured at 10 GHz. As shown in the figure, the ferroelectric transition appears at 233, 290, 285, and 290 K for annealed 100 Å, annealed 200 Å, annealed 500 Å, and as-deposited 500-Å-thick films, respectively, which are just below room temperature except that of the 100-Å-thick $SrTiO_3$ film. This is why the $SrTiO_3$ films exhibit abnormal nonlinear dielectric properties with a high dielectric constant and dielectric tuning as shown in Fig. 4(a). Also, the phase-transition peak for as-deposited 500-Å-thick film (i.e., 290 K) is observed to shift to a lower temperature (i.e., 285 K) after the annealing process [Fig. 5(a)]. This is the reason that the as-deposited $SrTiO_3$ film shows a higher dielectric constant and dielectric tuning than the annealed $SrTiO_3$ film at room temperature [Fig. 4(a)]. Even though it is not clear why the phase-transition peak for the annealed film appears at a lower temperature, presumably it is due to the possible annealing effects such as relaxed film strain and reduced oxygen vacancies, which are expected to

[This article is copyrighted as indicated in the article. Reuse of AIP content is subject to the terms at: http://scitation.aip.org/termsconditions. Downloaded to] IP: 128.84.143.26 On: Tue, 16 Jun 2015 17:09:37

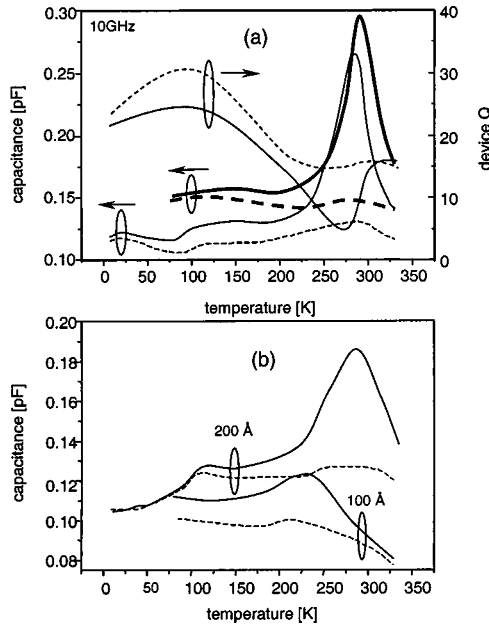

FIG. 5. (a) Capacitance and device Q of annealed $SrTiO_3$ thin film (500-Å thick) as a function of temperature and dc bias voltages (0 V for lines and 40 V for dot lines) at 10 GHz (also, the capacitance of as-deposited film is plotted with thicker lines) and (b) the capacitance of annealed $SrTiO_3$ films with other thickness (100-Å and 200-Å thick).

cause a reduced in-plane lattice constant. A typical device Q at 0 V dc bias of $SrTiO_3$ films [Fig. 5(a)] shows a maximum value from 30 to 40 at 110 K and a minimum value from 10 to 20 at 275 K, which is associated with the phase-transition peak. The device Qs of the films, which look too low to be applied to real devices, is believed to be mostly due to the dielectric Q ($=1/\tan\delta$) because any other loss factors (i.e., electrode conduction, leakage current, and substrate dielectric) are expected to be much lower compared to the dielectric loss in the film. Figure 4(b) shows the dielectric loss ($\tan\delta$) of as-deposited $SrTiO_3$ thin films (500-Å thick) as a function of applied dc bias measured at 10 GHz and room temperature. Actually, the room-temperature dielectric loss [Fig. 4(b)] is significantly higher (i.e., 0.19 at 0 V) compared with the other $SrTiO_3$ films, which are deposited on MgO or $LaAlO_3$ substrates whose phase transition occurs at very low temperatures (i.e., <50 K). We observed that the room-temperature dielectric loss for those $SrTiO_3$ films (i.e., deposited on MgO or $LaAlO_3$) was less than 0.005 at 0 V with no dielectric tuning in our previous research work. Presumably, the room-temperature high dielectric loss of the $SrTiO_3$ films deposited on $DyScO_3$ substrates is due to the film strain and well-oriented film microstructure (i.e., epitaxy) associated with a large electric polarization close to the phase-transition peak. This is because the total electric polarization in the film depends on the magnitude of the dipole moment formed in the unit cell, which is associated with film strain, and the coupling of the dipoles with each other, which is related to film orientation. Therefore, the relatively high dielectric loss of the strained epitaxial $SrTiO_3$ films must be related to the motion of the resulting large dipole moments with rf signal. Also, it is worth noting that the dc bias dependence of the dielectric loss [Fig. 4(b)] shows two patterns clearly; at a lower voltage the dielectric loss is decreased, and at a higher voltage the loss is increased. The dc bias dependence must be related also to the phase-transition peak even though how the actual loss mechanisms are related to the phase transition is not clear at this point. In Fig. 5(a), the dc bias dependence of the device Q ($\approx 1/\tan\delta$) of the annealed $SrTiO_3$ thin film (500-Å thick) changes at a region of the paraelectric phase close to the phase-transition peak. Below this region (i.e., ferroelectric phase) the device Q increases with dc bias, and above this region (i.e., paraelectric phase) the Q decreases with dc bias. This is why the dielectric loss at room temperature [Fig. 4(b)] is observed with two different dc dependencies.

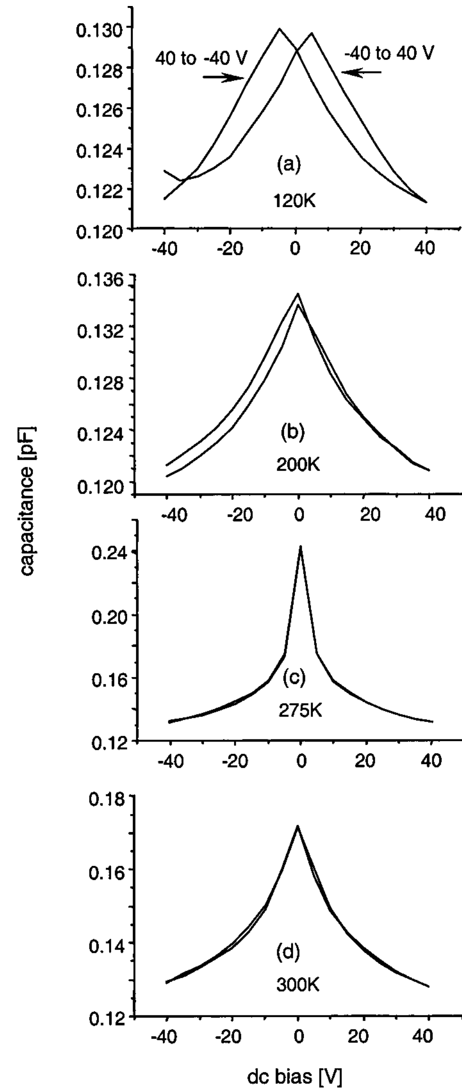

FIG. 6. Capacitance of $SrTiO_3$ thin film (500-Å thick) as a function of dc bias voltages at different temperatures (a) 120, (b) 200, (c) 275, and (d) 300 K at 10 GHz.

Figure 6 shows the capacitance of annealed 500-Å-thick $SrTiO_3$ film as a function of dc bias voltages (i.e., -40 to 40 V and 40 to -40 V with a 5 V step) at several different temperatures (i.e., 120, 200, 275, and 300 K) before and after the phase-transition peak (i.e., 285 K). Through temperature-dependent $C-V$ measurements, we may get an idea about how the films experience the ferroelectric phase

[This article is copyrighted as indicated in the article. Reuse of AIP content is subject to the terms at: http://scitation.aip.org/termsconditions. Downloaded to] IP: 128.84.143.26 On: Tue, 16 Jun 2015 17:09:37

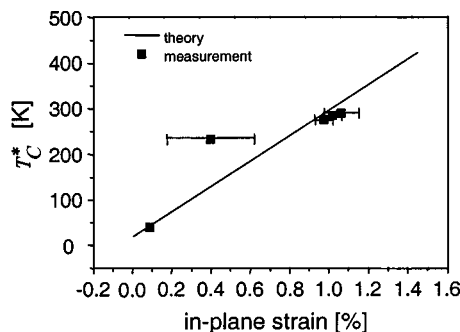

FIG. 7. Theoretical phase-transition peak as a function of film strain including experimental data [one of the measurements (i.e., $T_C^*=35$ K with 0.1% film strain for $SrTiO_3$ film on (001)MgO) is included from our previous work].

transition over the temperature range. As it is expected, the $C-V$ curve above the phase-transition peak do not exhibit any hysteresis because the film is supposed to be in a paraelectric phase (i.e., 300 K). However, it is interesting that the $C-V$ curve at 200 K, which is supposed to be in a ferroelectric phase just below the phase-transition peak, does not show a clear hysteresis, while the plot at 120 K, which is in a well below the phase-transition peak, shows a clear hysteresis behavior because of the ferroelectric phase. This may indicate the nature of the formation of the permanent dipoles in the $SrTiO_3$ films at the phase-transition peak (i.e., order of the phase transition). The order of the phase transition is determined by whether the onset of spontaneous polarization from zero to a finite value is continuous or discontinuous with respect to temperature.[23] Therefore, in the $SrTiO_3$ films, the phase transition may not be a first-order but a second-order phase transition, in which the permanent dipoles develop gradually rather than abruptly at the phase-transition peak.

Previously, we reported a theoretical analysis of the dielectric properties of epitaxial BST films[15] based on Devonshire's phenomenological theory.[23,24] Figure 7 shows a theoretical phase-transition peak as a function of film strain with some measured data of the $SrTiO_3$ films. The theoretical expression between the strain-induced phase-transition peak, T_C^*, and the film strain, x (i.e., in-plane strain for our measurement configuration) can be easily derived from the previous report as $T_C^*=T_C-2\varepsilon_0 C\{G_{11}x_1+G_{12}(x_2+x_3)\}$ where $x_3=-2c_{12}/c_{11}x_1$ and $x_1=x_2$, and T_C is the phase-transition temperature of $SrTiO_3$ with no strain. The relevant parameters in the expression can be found elsewhere.[15] It is also noted that the in-plane film strain used in Fig. 7 is estimated from the measured normal lattice parameter because of its better accuracy (Table II). As shown in the figure, even though the measured phase-transition peak is not well matched to the peak expected from the theory and the film strain, the phase-transition peak can be predicted well as a function of film strain for the ~1% strained films (⩾200-Å thick), whose strain measurements show higher accuracy.

IV. SUMMARY

We have investigated the microwave tunable dielectric properties of strained $SrTiO_3$ films. It was verified both experimentally and theoretically that the $SrTiO_3$ film strain of ~1% is sufficient to increase the temperature of the phase-transition peak up to approximately room temperature. The resulting large dielectric constant (i.e., 6000) and dielectric tuning (i.e., 75% at 1 V/μm) at 300 K should facilitate the use of strained $SrTiO_3$ in room-temperature tunable microwave applications.

[1] C. H. Mueller, R. R. Romanofsky, and F. A. Miranda, IEEE Potentials **20**, 36 (2001).
[2] S. S. Gevorgian and E. L. Kollberg, IEEE Trans. Microwave Theory Tech. **49**, 2117 (2001).
[3] D. S. Korn and H.-D. Wu, Integr. Ferroelectr. **24**, 215 (1999).
[4] T. Sakudo and H. Unoki, Phys. Rev. Lett. **26**, 851 (1971).
[5] R. C. Neville, B. Hoeneisen, and C. A. Mead, J. Appl. Phys. **43**, 2124 (1972).
[6] K. A. Muller and H. Burkard, Phys. Rev. B **19**, 3593 (1979).
[7] F. W. Van Keuls *et al.*, Appl. Phys. Lett. **71**, 3075 (1997); D. Fuchs, C. W. Schneider, R. Schneider, and H. Rietschel, J. Appl. Phys. **85**, 7362 (1999).
[8] W. J. Merz, Phys. Rev. **78**, 52 (1950).
[9] J. C. Slater, Phys. Rev. **78**, 748 (1950).
[10] P. W. Forsbergh, Jr., Phys. Rev. **93**, 686 (1954).
[11] G. A. Samara and A. A. Giardini, Phys. Rev. **140**, A954 (1965).
[12] T. Schimizu, Solid State Commun. **102**, 523 (1997).
[13] N. A. Pertsev, A. G. Zembilgotov, and A. K. Tagantsev, Phys. Rev. Lett. **80**, 1988 (1998).
[14] W. Chang, J. S. Horwitz, J. M. Pond, S. W. Kirchoefer, and D. B. Chrisey, Mater. Res. Soc. Symp. Proc. **526**, 205 (1998).
[15] W. Chang, J. S. Horwitz, W. J. Kim, J. M. Pond, S. W. Kirchoefer, C. M. Gilmore, S. B. Qadri, and D. B. Chrisey, Integr. Ferroelectr. **24**, 257 (1999).
[16] N. A. Pertsev, A. K. Tagantsev, and N. Setter, Phys. Rev. B **61**, R825 (2000); N. A. Pertsev, A. K. Tagantsev, and N. Setter, *ibid.* **65**, 219901(E) (2002).
[17] W. Chang, S. W. Kirchoefer, J. M. Pond, J. S. Horwitz, and L. Sengupta, J. Appl. Phys. **92**, 1528 (2002).
[18] J. H. Haeni, C. D. Theis, and D. G. Schlom, J. Electroceram. **4**, 385 (2000).
[19] J. H. Haeni *et al.*, Nature (London) (to be published).
[20] J. A. W. Dalziel, J. Chem. Soc. 1993 (1959).
[21] X-ray diffraction JCPDS, Card No. 27-0204 for $DyScO_3$.
[22] S. S. Gevorgian, T. Martinsson, P. I. J. Linner, and E. L. Kollberg, IEEE Trans. Microwave Theory Tech. **44**, 896 (1996).
[23] A. F. Devonshire, Adv. Phys. **3**, 85 (1954).
[24] It is worth to note that the Gibb's energy expression to derive the T_C-x relationship took positive signs (i.e., +) for all electrostriction-related terms like the Devonshire expression (see Ref. 23) so that the relevant electrostriction coefficients had the opposite signs (i.e., $Q_{11}[\mathrm{m}^4/\mathrm{C}^2]=-0.10$ and $Q_{12}[\mathrm{m}^4/\mathrm{C}^2]=0.034$) to the case of a Gibb's energy expression containing negatively signed electrostriction-related terms.

[This article is copyrighted as indicated in the article. Reuse of AIP content is subject to the terms at: http://scitation.aip.org/termsconditions. Downloaded to] IP: 128.84.143.26 On: Tue, 16 Jun 2015 17:09:37